IEEE Access
Multidisciplinary ⋮ Rapid Review ⋮ Open Access Journal

Received 3 September 2025, accepted 22 September 2025,
date of publication 25 September 2025, date of current version 2 October 2025.

Digital Object Identifier 10.1109/ACCESS.2025.3614516

RESEARCH ARTICLE

Genetic Algorithm-Based Optimization Framework for Offshore Wind Farm Layout Design

ITALO FIRMINO DA SILVA, TELLES BRUNELLI LAZZARIN, (Senior Member, IEEE), LENON SCHMITZ, (Member, IEEE), AND ALISON R. PANISSON
Universidade Federal de Santa Catarina (UFSC), Florianopolis, Santa Catarina 88040-900, Brazil

Corresponding author: Alison R. Panisson (alison.panisson@ufsc.br)

This work was supported by the Coordination for the Improvement of Higher Education Personnel–CAPES (ROR identifier: 00x0ma614) for the Article Processing Charge for the publication of this research. This work was supported in part by the National Council for Scientific and Technological Development (CNPq); and in part by the National Fund for Scientific and Technological Development (FNDCT) of the Ministry of Science, Technology and Innovations (MCTI), Brazil, under Grant 407826/2022-0.

ABSTRACT Offshore wind farms have emerged as a crucial component of renewable energy generation, offering higher energy production rates due to stronger and more consistent wind conditions. However, these advantages come with significant installation and maintenance costs, necessitating comprehensive optimization analyses of wind farms projects to ensure economic feasibility and maximize energy output. One of the most significant challenges in this context is the effective placement of wind turbines within an offshore wind farm, considering the historic wind intensity and direction of candidate areas, along with the impact of wake effects. This study presents a framework that integrates a genetic algorithm to optimize wind farms layouts with a simulation tool for evaluating configurations of wind farm projects. In this paper, we describe the optimization module implemented with genetic algorithms. Our approach aims to facilitate layouts optimization analysis for wind farms during the project phase, focusing on maximizing overall energy output by minimizing wake interference among turbines. The proposed approach demonstrates high modularity and achieves competitive results compared to established benchmarks, highlighting the effectiveness of our framework for optimization analysis in wind farm projects.

INDEX TERMS Genetic algorithms, offshore wind farms, optimization.

I. INTRODUCTION

Sustainable development has become a critical global priority. One of the most significant efforts in advancing sustainability is the adoption of renewable energy sources, such as wind power. Among the alternatives for wind farms, offshore wind farms are often favored over onshore alternatives due to their operation in areas with higher wind speeds, lower turbulence, fewer spatial constraints, and reduced impact on residential populations [1]. However, the implementation of offshore wind farms requires comprehensive studies to identify suitable locations, as they involve substantial construction and maintenance costs [1]. Selecting an appropriate site requires a thorough understanding of the geological landscape, which may be constrained by naval activities and water depth, as well as long-term wind patterns to ensure both economic feasibility and environmental compatibility.

A key challenge in implementing offshore wind farms is optimizing turbines placement, e.g., defining the wind farm layout, while accounting for restricted areas and associated costs. Turbine positioning directly influences implementation costs and, more critically, the efficiency of energy production, as wake effects and turbine interactions can substantially decrease overall power output. Wake losses are estimated to account for 10-15% of Annual Energy Production (AEP) in

The associate editor coordinating the review of this manuscript and approving it for publication was Xiaodong Liang.

wind farms [2], leading to substantial energy deficit over the operational lifespan of a wind farm.

In this paper, we propose a modular framework for evaluating wind farm projects, enabling the modeling of various project-specific variables. The framework extends our previous work [3], and integrates two core components: (i) a genetic algorithm that explores different wind farm layouts to identify optimized configurations; and (ii) an interface to existing simulation tools [4], which allows the estimation of energy output by specifying customizable components, including historical wind data and turbine wake models. This approach evaluates the energy output of each layout generated by the genetic algorithm, facilitating the identification of optimal configurations suited to potential implementation sites. The study provides a comprehensive overview of the proposed framework and assesses the performance of the genetic algorithm in optimizing wind farm layouts with respect to energy production. Additionally, it presents a real case study on the Brazilian coast, selected due to its strong offshore wind resources, ongoing government initiatives to regulate and promote offshore projects, and the country's growing energy demand. These factors make Brazil a timely and relevant context for exploring the applicability of advanced optimization methods in offshore wind farm design.

II. RELATED WORK

Optimizing Wind Farm Lyout (WFLO) is a critical challenge in maximizing energy production and minimizing costs. Researchers have explored various optimization techniques, broadly categorized into GF and gradient-based approaches.

A. GRADIENT-FREE APPROACHES

Several GF methods have been employed to address the non-convex nature of the Wind Farm Layout Optimization (WFLO) problem. Particle Swarm Optimization (PSO) utilizes randomly initialized ''particles'' to navigate the complex solution space, effectively reducing the risk of convergence to local optima and enhancing energy output [5]. Similarly, Genetic Algorithms (GAs) have been adapted for this context. One notable approach employs a matrix-based representation, where binary matrices (1s indicating turbines and 0s indicating empty cells) significantly reduce computational time and improve optimization outcomes compared to traditional chromosome representations [6]. An extension of this idea, the Multi-Population Genetic Algorithm (MPGA), incorporates immigration and coevolution mechanisms, enabling the exchange of individuals between subpopulations and their simultaneous evolution. This fosters genetic diversity and helps preserve elite solutions [7].

Other prominent GF techniques include Discrete Exploration-Based Optimization (DEBO), a novel algorithm specifically developed for WFLO. DEBO features a greedy initialization phase that places turbines near the boundaries to reduce wake losses, followed by a local search refinement phase that iteratively relocates individual turbines. This method treats the wake model as a closed box and does not require gradient information [8]. The Generalized Pattern Search (GPS) is a deterministic, GF algorithm that modifies turbine positions using predefined pattern vectors. It adaptively adjusts its step size to balance global exploration and local refinement, with constraints managed via penalty functions [8].

The Covariance Matrix Adaptation Evolutionary Strategy (CMA-ES) is a stochastic, GF optimization method that dynamically adapts its sampling distribution based on a multivariate normal distribution. It employs adaptive penalty scaling, allowing for early exploration of infeasible solutions before gradually converging to feasible, high-performing layouts [8]. The Add–Remove–Move Greedy (ADREMOG) algorithm is a discrete, heuristic approach that relies on a fast Pre-Averaged Model to estimate the Annual Energy Production (AEP). It iteratively adds turbines and adjusts their positions to minimize wake losses, often benefiting from a multi-start strategy to achieve robust results [8]. Finally, the Discrete Perturbation Algorithm (DPA) is a straightforward yet effective method designed for industrial application. It operates on a discretized design space, introducing both directed and random perturbations to turbine positions to achieve continuous performance improvements over time [8].

B. GRADIENT-BASED AND HYBRID APPROACHES

Gradient-based methods, while powerful, often encounter difficulties due to the non-convex nature and prevalence of local optima in the Wind Farm Layout Optimization (WFLO) problem. The Pseudo-Gradient Method mitigates these challenges by representing turbine interactions through vectors proportional to wind speed deficits, effectively substituting traditional gradients to guide layout adjustments [9]. This approach is computationally efficient, as it reuses previously calculated values. However, its vulnerability to local optima often necessitates the use of a multi-start strategy or its application as a pre-/post-processing step [8].

The Sparse Nonlinear Optimizer with Wake Expansion Continuation (SNOPT+WEC) represents an enhanced gradient-based method designed to overcome local optima. It incorporates the Wake Expansion Continuation (WEC) technique, which artificially broadens wake widths to smooth the design space, thereby facilitating more effective navigation by SNOPT. The method employs algorithmic differentiation to compute exact gradients and addresses non-convex boundaries by initially optimizing within a simplified convex hull [8].

Hybrid approaches aim to leverage the complementary strengths of both GF and gradient-based strategies. The Genetic- and Gradient-Based Hybrid Algorithm (GA-GB) exemplifies this, utilizing a genetic algorithm for global exploration and turbine distribution, followed by a gradient-based optimizer (SNOPT) for fine-tuning turbine positions. This approach benefits from the decoupling of discrete and continuous aspects of the problem; however,

its sequential structure may limit its ability to exploit improvements that require simultaneous optimization of both layers [8].

C. OTHER RECENT DEVELOPMENTS

Recent research continues to advance the field of Wind Farm Layout Optimization (WFLO). In [10], the authors proposed a renovation-oriented strategy for offshore wind farms, focusing on integrating new turbines into aging farms while preserving existing layouts. Their framework employs a machine learning-based wake model alongside both heuristic and gradient-based algorithms, demonstrating the feasibility of increasing the turbine count by up to 50% with minimal reduction in Annual Energy Production (AEP). In [11], the authors introduced a nonlinear optimization model for offshore wind farm design that aims to maximize lifetime profit by strategically selecting turbine placements and internal cable connections while avoiding cable crossings. The model incorporates wake effects, energy losses, and infrastructure costs, highlighting the critical role of optimal substation placement.

In [12], the authors developed a novel three-dimensional (3D) Gaussian wake model for enhanced optimization accuracy, integrated with a Mixed-Discrete Particle Swarm Optimization (MDPSO) algorithm. Their results show improved accuracy compared to traditional 1D and 2D wake models and higher energy output from non-uniform layouts. In [13], the authors proposed a multi-objective WFLO (MO-WFLO) framework that simultaneously optimizes power generation and streamwise turbulence intensity, a key factor in turbine fatigue. Leveraging the NSGA-II algorithm, the framework effectively balances energy output and structural resilience. Finally, In [14], the authors evaluated the effectiveness of various optimization algorithms in mitigating wake effects, comparing five methods, two population-based and three single-point. Their findings suggest that, under certain conditions, random search can outperform more sophisticated methods in terms of both quality and efficiency. For scenarios involving strict layout density constraints, hybrid strategies are recommended.

Unlike mentioned studies that often focus solely on optimization techniques or specific aspects of the wind farm layout problem, our work introduces a comprehensive, modular framework for AI-driven analysis of offshore wind farm projects. While we adopt a Genetic Algorithm (GA) for layout optimization, demonstrating to achieve competitive results when compared to approaches in the literature (as shown in Section VI), our contribution extends beyond algorithmic performance. The proposed framework enables the specification of project-specific characteristics, such as turbine models, wind resource distributions, and wake effects, exploring compatibility with existing simulation tools. Furthermore, it integrates visualization components that enhance the interpretability of optimization outcomes, facilitating practical analysis and decision-making. This holistic approach aims to bridge the gap between theoretical optimization and real-world offshore wind farm planning.

III. OFFSHORE WIND FARMS

Offshore wind farms are a crucial component of the future expansion of wind energy, as offshore wind conditions present stronger and more consistent wind speeds than onshore sites [15]. However, offshore wind farms require significant installation and maintenance costs, which necessitates optimization efforts to maximize energy extraction from these high-cost installations. Thus, it is essential to conduct studies to select the most appropriate location for installing an offshore wind farm, taking into account the topography, naval activities, and, most importantly, the wind incidence in the available locations [16]. Furthermore, various offshore wind farm layouts must be considered, as they directly impact the farm's capacity to maximize energy production [17], [18], [19]. Maximizing energy production requires minimizing wake losses, a complex challenge influenced by numerous variables, including the historical wind speed and direction at a candidate location, area size, and the types of offshore turbines selected.

In addition to these technical challenges, cost optimization plays a critical role in the overall project feasibility. This includes evaluating the topologies for electrical cabling, where selecting the appropriate configuration (e.g., radial, star, or ring) can significantly impact both installation costs and operational efficiency [20]. The choice of components, such as offshore substations, transformers, and subsea umbilical cables, must also balance reliability and cost-effectiveness [21]. Furthermore, factors like distance from shore, seabed conditions and available infrastructure influence decisions on logistics, installation methods and long-term maintenance, all of which are essential to optimizing both the initial investment and energy yield over the lifetime of the wind farm.

A. WIND DISTRIBUTION

The wind resource distribution in candidate areas for offshore wind farms can be assessed through years of wind speed data sampling [2]. Normally, measured wind speed is represented using a probabilistic distribution model, which overlooks the uncertainty of wind power levels over extended time periods in wind farm planning and design [22]. This wind distribution model is then used as input for a wake model, considering wake losses based on the characteristics of the wind turbines used, to calculate the expected energy production output.

Figure 1 presents the wind distribution for the Mostardas-RS region on the Brazilian coast, which is later used as a real-world case study.

B. WAKE EFFECT

In the context of wind farms, a wake refers to a region of disturbed airflow. When the wind passes through the turbine blades, it forces them to rotate, generating mechanical energy,

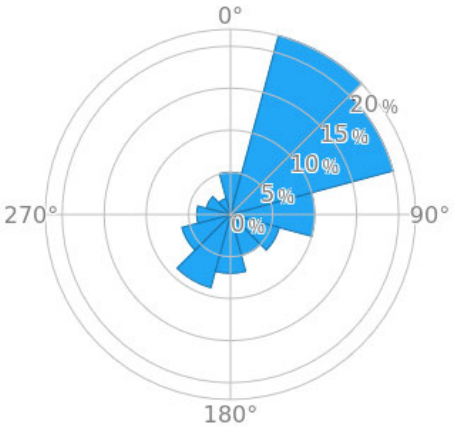

FIGURE 1. Wind distribution for Mostardas-RS on the Brazilian coast, based on Global Wind Atlas data.

which is then converted into electricity. However, the interaction of wind with the blades reduces its speed and increases turbulence in the area behind the turbine, known as the wake, which decreases the rotation of downstream turbines and, consequently, reduces overall energy production [15].

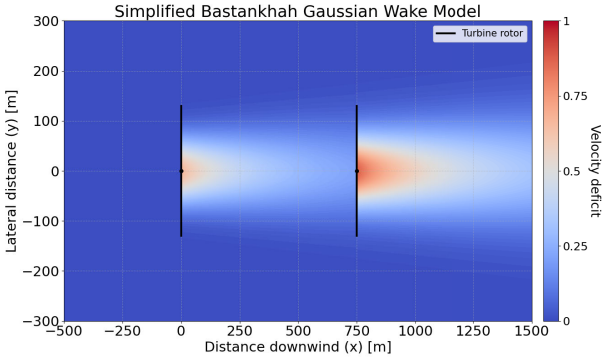

FIGURE 2. Detailed view of wake effect.

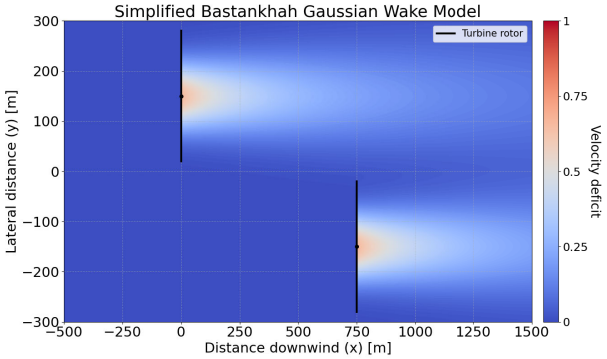

FIGURE 3. Detailed view of wake effect.

Studies indicate that the wake effect is influenced by the following factors: distance between the turbines, wind direction, rotational speed, blade angle, and the alignment

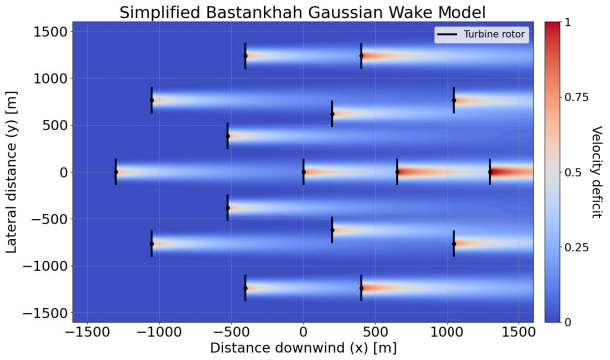

FIGURE 4. Overview of wake effect.

angle of the turbine with the wind [21]. The first two factors can be considered in the layout design of the wind farm, taking into account the prevailing wind direction in the installation area and the optimal spacing between turbines. The other three factors can be modified during operation and thus optimized to ensure the greatest possible power extraction without compromising turbine wear. Figures 2 and 3 illustrates the wake effect in a detailed view between two turbines, and Figure 4 an overview for a wind farm.

A wake model is suppose to take into account the characteristics of the wind turbines to estimate the wind speed and direction following its interaction with the turbine blades, and then predict the wind speed and direction for downstream turbines. Wake modeling can be categorized into two sorts [22]: (i) wake models using computational fluid dynamics (CFD) technology, which simulate the dynamics of wind flow characteristics with good accuracy, but requiring large amount of computational resources [23], [24]; and (ii) wake models using analytical models to estimate wind speed deficit [4], [25], [26], [27], [28].

Analytical wake models provide a simpler and more computationally efficient approach compared to CFD-based models. These models rely on mathematical formulations to describe the wind flow behavior behind turbines without the need for heavy simulations, making them more suitable for the development of decision-support tools for wind farm projects. One of the most widely used analytical models is Bastankhah's Gaussian wake model [27]. This model assumes a Gaussian distribution for the velocity deficit in the wake, allowing it to predict how the wind speed decreases downstream of a turbine. The simplified version of Bastankhah's model [4], [28] incorporates key factors such as wake expansion, turbulence intensity, rotor diameter, and the thrust coefficient of the turbine. Compared to classical approaches such as Jensen's model [29], the Gaussian formulation provides more accurate wake recovery and velocity deficit predictions while retaining low computational cost. Its balance between accuracy and efficiency makes it particularly suitable for wind farm layout optimization, enabling large-scale simulations with minimal computational

resources.

$$\frac{\Delta U}{U_\infty} = \left(1 - \sqrt{1 - \frac{C_T}{8\sigma_y^2/D^2}}\right) \exp\left(-0.5\left(\frac{y-\delta}{\sigma_y}\right)^2\right) \tag{1}$$

$$\sigma_y = (k_y \cdot x) + \frac{D}{\sqrt{8}} \tag{2}$$

Equation (1) represents the simplified Bastankhah's Gaussian wake model [4], [27]. In this equation, the wake velocity deficit, $\frac{\Delta U}{U_\infty}$, represents the reduction in wind speed caused by the wake from an upstream turbine. The term C_T is the turbine's thrust coefficient. The term $y - \delta$ is the lateral distance from the wake center, D is the turbine diameter, and σ_y is the standard deviation of the wake spread in the cross-stream direction. The wake spread σ_y is further defined by equation (2), with x being the downstream distance between the wake-generating turbine and the affected turbine. The parameter k_y is a function of turbulence intensity. The simplified Bastankhah's Gaussian wake model allows for the consideration of different turbines by adjusting the mentioned parameters. In Section VI, the values of these parameters and constant terms used in our study are discussed.

IV. OFFSHORE WIND TURBINE PLACEMENT PROBLEM

One of the most critical challenges in offshore wind farm projects is the layout design, as it affects not only installation costs but, more importantly, long-term energy production, which can be significant over time. Therefore, assessing the feasibility of an offshore wind farm requires careful analysis of potential sites, local wind distribution patterns, and the chosen turbine model, including its associated wake effects. This process involves evaluating various wind farm layouts to optimize energy output, taking all these factors into account.

To support this task, the authors in [4] have proposed a wind farm simulation tool, allowing to incorporate each mentioned variable and evaluate different layouts regarding the output energy production.

A. MODELING AND SIMULATION OF WIND FARM ENERGY PRODUCTION

Numerous tools have been developed to model and simulate energy production in wind farms. In [4], the authors present a wind farm simulation tool that enables configuration of: (i) various wake models based on turbine specifications; (ii) historical wind data for the candidate site; and (iii) multiple wind farm layouts. The simulator then estimates the expected energy output for the configured wind farm. Figure 5 illustrates an overview of the wind farm simulation tool component we incorporate in our framework.

Accurately modeling wake effects is fundamental for optimizing wind farm layouts, as it directly impacts energy production and overall performance. To explore this, the authors in [4] invited the wind energy and optimization community to contribute to a two-part study. In the first case study, participants were provided with all the necessary

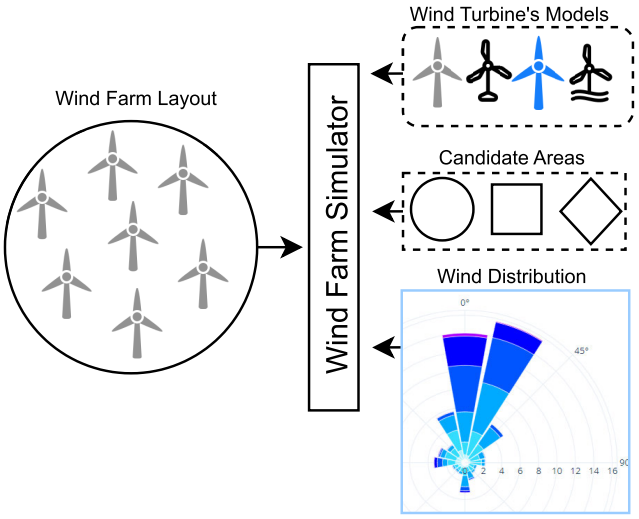

FIGURE 5. Overview for wind farm simulation.

functions to evaluate their proposed wind farm layouts based on predefined models. In contrast, the second case study allowed participants to choose their own wake model, whether analytic or Computational Fluid Dynamics (CFD), to simulate the wake effects between turbines. In this case, the results were evaluated through cross-validation, with participants assessing each other's optimized layouts under each wake model. The simulator, used to evaluate performance in the first case, takes as input a predefined turbine model and wind rose (probability distribution), both common to all participants, and the x, y coordinates of the turbines, which differ based on individual optimizations [4].

In this paper, we utilize the scenarios and benchmarks from [4], focusing on the first case study that employs an analytical technique for the wake model and predefined components. Our approach is evaluated by comparing our results against the benchmarks presented in [4].

B. VARIABLES

Originally, the simulator [4] takes into account the following inputs, divided into three main groups: (i) the turbine attributes group, which includes the cut-in and cut-out wind speeds representing the minimum and maximum wind speeds at which the turbine operates; the rated wind speed, at which the turbine reaches its maximum power output; the rotor diameter, which plays a role in modeling the simplified Bastankhah's wake effect; and the power curve, which determines how wind speed is converted into electrical energy; (ii) the wind resource group includes wind direction and its frequency distribution, modeling how often the wind blows from specific directions; and, (iii) the turbine location group, where the x and y coordinates of the turbines are used to calculate the distances between them, close turbines increases the wake effect due to wind interaction with upstream turbines.

By adjusting these inputs, it is possible to simulate the energy output of wind farm projects, including the evaluation of various wind farm layouts by altering the x and y coordinates of the set of turbines considered. Also, it is possible to consider different candidates area, distance between turbines, etc. These factors related to layout are not input variables of the simulator but can be modeled as constraints or optimization variables defined in the wind farm project.

V. AN OPTIMIZATION APPROACH USING GENETIC ALGORITHMS

In this section, we describe the component of our framework responsible for optimizing the wind farm layout, which is implemented using genetic algorithms. As shown in Figure 5, there are a substantial number of variables to consider when evaluating the performance of potential wind farms projects.

To evaluate the optimization component, this paper will focus only on varying the input for the wind farms layouts in the simulator, considering exclusively the wake effects. The evaluation is conducted within a fixed candidate area, utilizing the wind history of that location and a predefined turbine model. Thus, it can be compared with the benchmark results presented in [4].

A. OPTIMIZATION PROBLEM

A classical optimization problem aims to minimize (or maximize) an objective function [30], which represents the fitness of potential solutions. The objective function, $f(x)$, depends on a set of decision variables, $x = [x_1, x_2, \ldots, x_n]$, and evaluates the quality of each solution. The optimization is subject to constraints that define the feasible region, including equality constraints $g_i(x) = 0$ and inequality constraints $h_j(x) \leq 0$ [30]. These constraints ensure that the solution adheres to specific requirements, such as physical limitations or resource availability.

In this study, the fitness function is defined as the Annual Energy Production (AEP), presented in equation (3). The parameter N represents the number of wind directions considered, which, in our study, as usually, has been discretized into 16 distinct directions. The term f_i denotes the frequency of wind blowing from a specific direction i, and P_i^{farm} is the total power produced by the wind farm when the wind comes from that direction. The factor $8760\frac{\text{hrs}}{\text{yr}}$ corresponds to the total number of hours in a year, calculated based on a standard year of 365 days with 24 hours per day.

$$AEP = \left(\sum_{i=1}^{N} f_i P_i^{farm}\right) 8760 \frac{\text{hrs}}{\text{yr}} \tag{3}$$

To obtain the total power of the wind farm, P_i^{farm}, the powers from all n turbines are summed, according to equation (4).

$$P_i^{farm} = \sum_{j=1}^{N} P_j^{turb} \tag{4}$$

The power curve and the wind speed, ve, are utilized to calculate each turbine's power output through a piecewise formulation that models its performance under varying wind conditions:

$$P^{turb}(ve) = \begin{cases} 0 & ve < V_{cut-in} \\ P_{rated} \cdot \left(\dfrac{ve - V_{cut-in}}{V_{rated} - V_{cut-in}}\right)^3 & V_{cut-in} \leq ve < V_{rated} \\ P_{rated} & V_{rated} \leq ve < V_{cut-out} \\ 0 & ve \geq V_{cut-out} \end{cases} \tag{5}$$

Here, $V_{\text{cut-in}}$, V_{rated}, and $V_{\text{cut-out}}$ represent the cut-in, rated, and cut-out wind speeds, respectively, while P_{rated} is the turbine's maximum power output. Below $V_{\text{cut-in}}$, no power is produced. Between $V_{\text{cut-in}}$ and V_{rated}, the power increases cubically. Beyond V_{rated} and up to $V_{\text{cut-out}}$, the turbine produces constant rated power, shutting down at higher wind speeds to prevent damage. The velocity is initially set to a constant 9.8 m/s, which is the turbine's rated wind speed. This is a strategic feature of the benchmark design [4], forcing any waked turbine onto the steepest part of its power curve, it creates a complex fitness landscape with numerous local optima, providing a more robust test for optimization algorithms. The reduction in velocity is attributed to the wake effect, described by equation (1), which reflects the wind speed ve.

Consequently, the problem is formulated as an optimization task to maximize the AEP of the wind farm, represented by the function AEP, considering a set of n turbines $[(x_1, y_1), \ldots, (x_n, y_n)]$ and the wake effects arising from their relative positioning. The optimization is subject to two constraints:

1) the distance between any two turbines, (x_i, y_i) and (x_j, y_j), must be at least twice the rotor diameter, $2D_r$, to minimize wake interference;
2) all turbines must be located within the bounds of a circular area, ensuring $(x_c - x_i)^2 + (y_c - y_i)^2 \leq R_b^2$, in which R_b is the radius of the farm boundary.

B. PROBLEM MODELING AND SIMULATOR INTEGRATION

Our methodology involves configuring predefined information about a candidate area, its wind probability distribution, and the turbine model within the simulator presented in Figure 5, originally proposed in [4]. These variables were defined based on those used in the first case study from [4], which serves as a benchmark for comparison with our results.

To explore the layout optimization space, we employ a genetic algorithm that generates and evaluates various wind farm configurations. The simulator is integrated into this process, using the AEP as the fitness function, where higher energy output corresponds to a higher fitness value.

Each agent (i.e., an individual in the algorithm's population) represents a candidate wind farm layout.

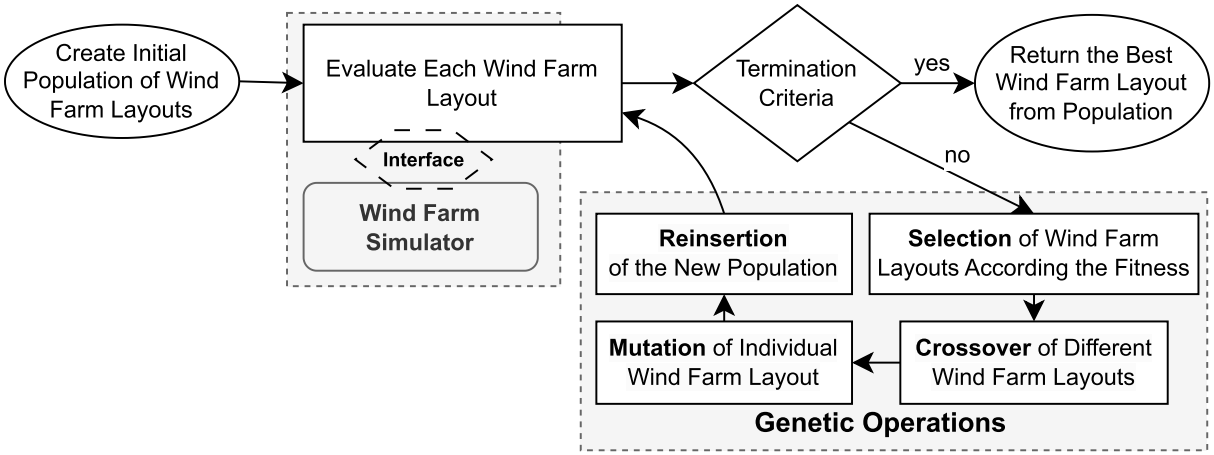

FIGURE 6. Proposed evolutionary approach.

Specifically, each agent is encoded as a vector of coordinates, $[(x_1, y_1), (x_2, y_2), \ldots, (x_n, y_n)]$, where (x_i, y_i) denotes the position of the i-th turbine, and n is the number of turbines in the configuration. This representation is compatible with the simulation tool described in Section IV-A, allowing accurate evaluation of each layout's energy output and guiding the search toward more efficient configurations.

The proposed approach applies the following genetic operations, adapted to the wind farm layout optimization problem [31]:

- **Selection**: Prioritizes better-performing agents, allowing them to reproduce more frequently than less fit ones. From the current population of candidate layouts, a subset is selected to undergo crossover and mutation.
- **Crossover**: Exchanges genetic information between selected agents to create new candidates. By combining turbine positions from different parent layouts, new configurations are generated that inherit potentially beneficial traits from both.
- **Mutation**: Introduces random modifications to an agent's structure, such as repositioning turbines within the layout. This promotes diversity in the population and helps avoid premature convergence to suboptimal solutions.

Our GA is distinguished from a basic implementation through several adaptations tailored to the WFLO problem. Most notably, it employs a hybrid constraint-handling strategy: a repair mechanism projects any turbine placed outside the farm boundaries back to the nearest valid position, while a penalty function reduces the fitness of layouts that violate the minimum inter-turbine distance constraint. This is complemented by a Gaussian mutation operator, which is more effective than standard mutation for fine-tuning turbine positions in a continuous space.

At the simulation level, the following components are modeled through configurable modules: (i) candidate area constraints; (ii) wake model and associated turbine characteristics; and (iii) wind speed and directional data for the target region. The genetic algorithm is integrated with the simulator such that each candidate layout is evaluated by invoking the simulator to estimate its AEP. This seamless integration enables an automated and flexible pipeline for layout optimization. Figure 6 illustrates the proposed process.

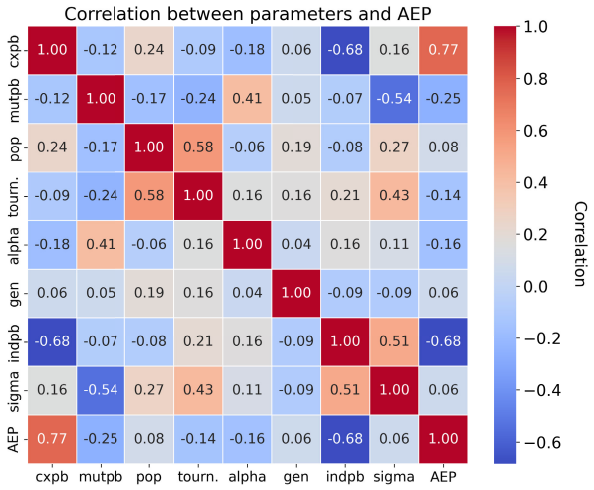

FIGURE 7. Correlation map.

VI. EVALUATION

To evaluate our approach, we considered the 3 optimization problems from [4], contrasting our results to the benchmarks collected from participants by the authors. In Section VI-A, we describe a set of experiments conducted to understand the correlation between the parameters of the genetic algorithm. Based on these experiments, we define the parameters and the range of values to be explored in our hyperparameterization approach. In Section VI-C, we then execute the proposed method to the 3 optimization problems from [4], comparing the results obtained.

A. PARAMETRIZATION

A common challenge when using evolutionary algorithms, such as genetic algorithms, is selecting the appropriate parameters to guide the algorithm toward optimal solutions while avoiding premature convergence [32].

The genetic algorithm implemented in our approach utilizes the following parameters [33]: *population*, which specifies the size of the agent population; *cxpb* (crossover probability), which represents the likelihood of two agents being mated; *ngen*, the maximum number of generations; and *mutpb* (mutation probability), which denotes the probability of an agent undergoing mutation. Additionally, when either a mating or mutation event occurs, further parameters must be considered. In case of mating, the parameter *alpha* determines the proportion of genetic material exchanged between agents. In case of mutation, the parameter *indpb* (individual probability) regulates the extent to which the genetic material of a single agent is subject to mutation. When a mutation occurs, affecting either a specific gene or the entire genetic sequence, a random value is sampled from a Gaussian distribution characterized by a mean of μ and a standard deviation of σ, which is subsequently added to the gene. The selection genetic operator employed is the *tournament* method, which selects the best-fit agent from a pool of k agents. These parameters collectively govern the evolutionary process, influencing the convergence and diversity of solutions within the population.

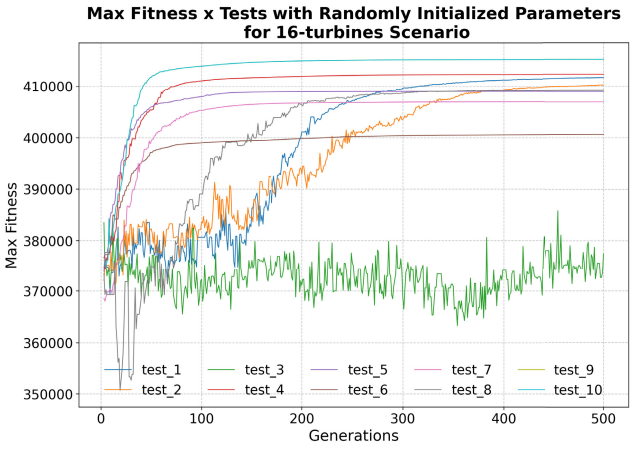

FIGURE 8. Search behaviour.

To understand the correlation between these parameters for this specific problem, we conducted 18 experiments, a sample size confirmed as sufficient by a *post-hoc* statistical power analysis [34], [35]. For the strongest observed correlations (r = 0.77 and r = -0.68), the analysis yielded a statistical power of 98% and 91%, respectively (α=0.05). These trials involved configuring the parameters randomly across different ranges to extract both positive and negative correlations, as shown in Figure 7.

Table 1 shows the 18 experiments conducted. Also, Figure 8 illustrates the algorithm's performance across 10 of the conducted experiments, in which each line represents a different experiment, selected from the 18 experiments in Table 1, demonstrating how the variety of parameters explored in these experiments influences both the search space and the performance of the algorithm. This highlights the sensitivity of the algorithm's behavior to the initial parametrization and emphasizes the diversity of experiments used to understand the correlations among the algorithm's parameters.

TABLE 1. Genetic algorithm parameters and AEP (MWh).

ID	cxpb	mutpb	Pop	Tourn	Alpha	Gen	indpb	sigma	AEP
1	0.7	0.3	100	2	0.5	1000	0.2	50	411815
2	0.8	0.4	100	2	0.5	1000	0.2	50	411936
3	0.85	0.45	100	2	0.5	1000	0.2	50	410619
4	0.85	0.45	250	2	0.5	1500	0.2	50	411012
5	0.8	0.4	250	4	0.5	1500	0.2	50	412294
6	0.8	0.4	250	5	0.6	2500	0.2	50	410555
7	0.5	0.45	250	6	0.6	1500	0.35	50	400872
8	0.8	0.4	250	3	0.5	2000	0.15	10	407065
9	0.8	0.4	250	4	0.75	1500	0.3	150	409235
10	0.7	0.3	250	4	0.4	1500	0.4	150	404785
11	0.8	0.4	500	4	0.5	3500	0.2	50	410847
12	0.85	0.35	250	5	0.5	3500	0.2	100	412741
13	0.85	0.35	300	5	0.5	500	0.2	100	415203
14	0.85	0.35	500	5	0.5	500	0.2	100	411113
15	0.85	0.35	400	5	0.5	500	0.2	100	412403
16	0.85	0.35	300	5	0.5	3000	0.2	100	415289
17	0.85	0.35	350	5	0.5	2500	0.2	100	410840
18	0.85	0.35	300	6	0.5	1000	0.2	100	408632

The previous correlation analysis indicated that *cxpb* had a strong positive correlation with AEP (0.77), while *indpb* exhibited a significant negative correlation (−0.68), and *mutpb* showed a weaker negative correlation (−0.25). Based on these findings, a hyperparameter search was conducted by varying *cxpb*, *indpb*, and *mutpb* within the continuous range of 0 to 1, in increments of 0.05. The remaining parameters were arbitrarily fixed during the hyperparameter tuning. This strategy allowed for refining the parameter values to optimize AEP.

B. CODE PROFILING AND OPTIMIZATION

The wind-farm optimization code was profiled using Python's `cProfile`, revealing that four functions—particularly `GaussianWake`—dominated runtime. This insight directed optimization efforts toward improving the wake calculation, which initially relied on deeply nested loops.

To accelerate computation while preserving the physical accuracy of the model, four key techniques were applied: (1) vectorization using NumPy broadcasting to replace nested loops with array operations, (2) boolean masking to efficiently filter downstream turbine pairs, (3) pre-allocation of working arrays to reduce memory overhead, and (4) parallelization of fitness evaluations using Python's multiprocessing module.

The wake calculation was reformulated using NumPy arrays to compute turbine separations and wake deficits in

bulk, avoiding Python-level loops. This approach not only preserved the physical model's integrity but also dramatically increased computational efficiency. The final vectorized formulation computes wake losses per turbine using matrix operations, enabling fast, large-scale evaluations.

Performance comparisons demonstrated the impact of these optimizations. A benchmark involving a 100-turbine layout optimized over 50 generations showed a runtime reduction from 57 minutes to just 18 seconds, yielding a 190× speedup (99.47% faster) on a 12-core Intel Core i5 system running Ubuntu Linux.

C. RESULTS

To evaluate our framework and compare our results with the benchmark available in [4], we use the same wake model employed by other participants, applying the following constants in the wake model equations (1) and (2).

- Thrust coefficient (C_T): 8/9.
- Rotor turbine diameter (D): 130m.
- k_y, relating to a turbulence intensity of 0.075: 0.0324555.

Also, we used the same 3 optimization problems for wind farm layout from [4], comprising 16, 36, and 64 turbines, placed within circular sites of 1300, 2000, and 3000 meters in radius, respectively. As a result of those code optimizations explained in section IV, we were able to perform a broad range grid search over 8000 parameter combinations (crossover probability, mutation probability and individual mutation probability each varying from 0.05 to 1.00 in 0.05 increments) in feasible time. These parameters were selected based on their correlation with the AEP, as shown in Figure 7. The remaining algorithm parameters were chosen arbitrarily. The best parameters for each scenario are gathered in Table 2.

TABLE 2. Final GA parameters for the different scenarios.

Turb.	cxpb	mutpb	Pop	Tourn	alpha	Gen	indpb	sigma	mu
16	0.95	0.70	300	5	0.5	1500	0.40	100	0
36	1.00	0.35	300	5	0.5	1500	0.10	100	0
64	0.80	0.20	300	5	0.5	1500	0.20	100	0

TABLE 3. Comparative results for the 16 turbines scenario.

Rank	Algorithm	Grad.	AEP (MWh)	Increase
1	Our Approach	GF	419,500	14.32%
2	SNOPT+WEC	G	418,924	14.17%
3	Our Previous Approach	GF	416,897	13.61%
4	fmincon	G	414,141	12.86%
5	SNOPT	G	412,251	12.35%
6	SNOPT	G	411,182	12.06%
7	PSQP	G	409,689	11.65%
8	Multistart Interior-Point	G	408,360	11.29%
9	Full Pseudo-Gradient Approach	GF	402,318	9.64%
10	Basic Genetic Algorithm	GF	392,587	6.99%
11	Simple PSO	GF	388,758	5.95%
12	Simple Pseudo-Gradient Approach	GF	388,342	5.83%
13	(Example Layout)	-	366,941	-

The power produced by each wind turbine (fitness) is evaluated according to the equation (3) [4]. Under ideal conditions, the annual energy production (AEP) for a given wind farm configuration is calculated by summing the individual contributions of each turbine's power output over 8,760 hours (representing one year). Thus, the resulting maximum AEP values for each optimization problem are 469,536 MWh, 1,056,456 MWh, and 1,878,144 MWh for 16, 36 and 64 turbines, respectively.

TABLE 4. Comparative results for the 36 turbines scenario.

Rank	Algorithm	Grad.	AEP (MWh)	Increase
1	Our Approach	GF	863,786	17.06%
2	SNOPT+WEC	G	863,676	17.05%
3	Our Previous Approach	GF	854,895	15.85%
4	Multistart Interior-Point	G	851,631	15.42%
5	PSQP	G	849,369	15.11%
6	SNOPT	G	846,357	14.70%
7	SNOPT	G	844,281	14.42%
8	Full Pseudo-Gradient Approach	GF	828,745	12.31%
9	fmincon	G	820,394	11.18%
10	Simple Pseudo-Gradient Approach	GF	813,544	10.25%
11	Basic Genetic Algorithm	GF	777,475	5.37%
12	Simple PSO	GF	776,000	5.17%
13	(Example Layout)	-	737,883	-

TABLE 5. Comparative results for the 64 turbines scenario.

Rank	Algorithm	Grad.	AEP (MWh)	Increase
1	SNOPT+WEC	G	1,513,311	16.86%
2	PSQP	G	1,506,388	16.36%
3	Our Approach	GF	1,488,203	14.92%
4	Multistart Interior-Point	G	1,480,850	14.35%
5	Our Previous Approach	GF	1,479,753	14.26%
6	SNOPT	G	1,476,689	14.03%
7	Full Pseudo-Gradient Approach	GF	1,455,075	12.36%
8	SNOPT	G	1,445,967	11.66%
9	Simple Pseudo-Gradient Approach	GF	1,422,268	9.82%
10	Simple PSO	GF	1,364,943	5.40%
11	fmincon	G	1,336,164	3.18%
12	Basic Genetic Algorithm	GF	1,332,883	2.93%
13	(Example Layout)	-	1,294,974	-

Tables 3, 4, and 5 present the AEP values obtained by our approach for each optimization problem, ranked alongside those reported by other participants in [4], and our previous results reported in [3]. Among the ten solutions reported in the study [4], six employ gradient-based (G) approaches and four utilize Gradient-Free[1] (GF) methods. Additionally, one layout (13th row in the tables) corresponds to an example provided by the authors of [4], while another solutions, highlighted in orange and yellow, represents our genetic algorithm-based approach before and after code optimization, respectively, categorized as a GF method. Our method demonstrated strong and consistent performance across all scenarios, achieving AEP values that placed the genetic algorithm competitively among the best-performing solutions.

Notably, in the 16-, 36-, and 64-turbine scenarios, our algorithm achieved AEP increases of 14.32%, 17.06%, and 14.92%, respectively, compared to the example layout provided by the authors of [4]. Our solution ranked first in both the 16- and 36-turbine scenarios, and secured third

[1]Gradient-based methods leverage function gradients for faster convergence, whereas GF methods operate without relying on gradients, making them suitable for complex or non-differentiable problems.

place in the 64-turbine case. When considering only other GF methods, our approach outperformed all competing solutions across the three optimization scenarios. Relative to the maximum theoretical energy output for each turbine configuration, our approach achieved 89.34%, 81.76%, and 79,23% of the maximum AEP for the 16-, 36-, and 64-turbine scenarios, respectively. In comparison, the method reported in [4] (SNOPT+WEC) reached 89.22%, 81.75%, and 80.57% for the same scenarios. This deviation from maximum generation is observed across all methods and is attributed to the spatial constraints imposed by the limited area relative to the number of turbines. These results highlight the potential of genetic algorithms to consistently deliver optimal or near-optimal solutions for complex optimization problems [31], particularly in the context of renewable energy systems design. Furthermore, they validate the effectiveness of the optimization component within the proposed framework.

VII. REAL CASE STUDY-BRAZILIAN COST

To validate the proposed framework in a realistic context, we conducted a case study focused on a potential offshore wind farm site near Mostardas, in the southern coast of Rio Grande do Sul, Brazil. The selected area covers approximately 225 km^2 and was chosen based on analyses provided by the Brazilian Institute of Environment and Renewable Natural Resources in [36]. According to data from the Global Wind Atlas,[2] the region exhibits favorable wind conditions, with high wind speeds, as showed in Figure 10, and good power density, as showed in Figure 9, making it a promising candidate for offshore wind energy generation in the Brazilian coast.

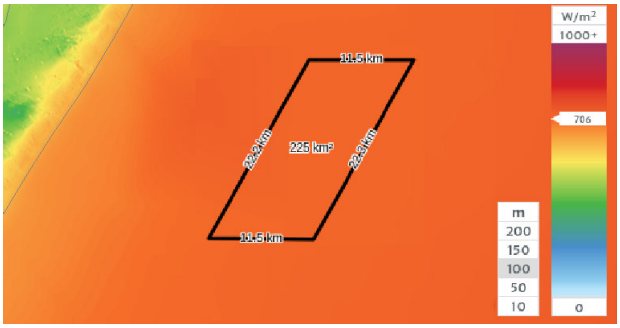

FIGURE 9. Power density map of the selected area near Mostardas-RS, based on Global Wind Atlas data.

According to a previous viability study in this same area, we employed the IEA 15MW reference wind turbine model, with detailed specifications such as rated power, nominal wind speed, and operational cut-in and cut-out thresholds, as documented by NREL [37]. The following section details the application of our optimization framework to this real-world scenario, which provides a comprehensive evaluation for a wind farm implementation is the mentioned area.

[2]https://globalwindatlas.info/en/

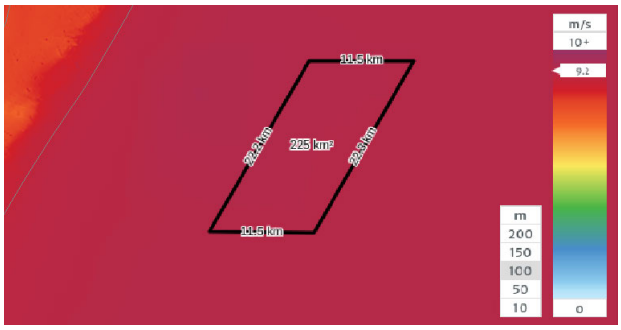

FIGURE 10. Average wind speed distribution in the study area, according to Global Wind Atlas data.

A. REAL CASE MODELING

Given the robustness and modularity of the proposed framework, modeling the real-world case near Mostardas-RS was a straightforward process, following the same configuration strategy adopted in Section VI. The framework's architecture allowed us to quickly adapt key components through configuration files without altering the core optimization logic, with efficiency already validated.

The wind conditions for the selected area were obtained from the Global Wind Atlas, which provides a wind rose with frequency and directional data, as showed in Figure 1. Although the tool does not offer direct access to tabular data, it allows approximate values to be extracted by interacting with the graphical interface. These frequency and direction values were manually inserted into the framework component towards a YAML configuration file.

The wind farm implementation project for Mostardas-RS is expected to use the IEA 15 MW turbine model. Its technical specifications, such as nominal wind speed, cut-in and cut-out speeds, and rotor diameter, were defined within the corresponding module of the framework and configured via a YAML file. This configuration enabled the simulation component to accurately model wake interactions and energy generation behavior based on realistic turbine characteristics, as well as the wind speed and direction data of the selected implementation area. In addition, the geographic boundaries of the optimization region were defined within the framework using a simple polygonal representation.

After adjusting the project-specific inputs in the framework, the system computes the optimized turbine placement using the approach described in Section V. This process is implemented through a genetic algorithm that evaluates a population of wind farm layouts, ultimately selecting the configuration with the highest estimated energy output.

During the optimization process, the proposed approach employs the nominal wind speed of the selected turbine model. This choice is strategic for creating the most effective fitness landscape for the optimization algorithm. Optimizing at low wind speeds provides a weak fitness signal, as the minimal absolute power deficit caused by wakes makes it difficult for the algorithm to distinguish between high-performing and

low-performing layouts, hindering its convergence to a truly optimal solution. Conversely, at speeds above nominal, the wake effect becomes invisible as the turbine's output is fixed at its maximum rated power. Therefore, the nominal speed maximizes the contrast in fitness between different layouts, providing the clearest information to guide the algorithm. This methodology is also consistent with the benchmark study discussed in Section VI. After the optimized layout is obtained, the AEP is then calculated using the actual wind speed data from the implementation area.

To explore the potential AEP of the selected area, several wind farm configurations were simulated by varying the number of turbines. This document presents the evaluation of projects containing 60, 80, 100, and 150 turbines. For the configuration with 150 turbines, each individual layout comprises 300 coordinate values, making hard-coded definitions both impractical and error-prone. To address this, the initial turbine positions and placement bounds were specified via configuration files integrated into the proposed framework.

This modeling approach highlights the flexibility of the framework, enabling the evaluation of real-world offshore wind scenarios with minimal manual intervention and high adaptability to different turbine models and site-specific characteristics.

B. RESULTING OPTIMIZED LAYOUT

After obtaining an optimized wind farm layout based on the project-specific characteristics, the expected AEP for each configuration was calculated using the actual wind speed distribution from the Global Wind Atlas, as shown in Figure 10. The results for projects with 60, 80, 100, and 150 turbines at the selected site near Mostardas-RS are presented in Table 6.

The output optimized layout configurations are depicted in Figures 12, 13, 14 and 15 for the projects of 60, 80, 100 and 150 turbines, respectively. Figure 11 shows the visual output of the simulation model, allowing a visual inspection by engineers.

TABLE 6. Comparison between ideal and optimized energy output for different turbine configurations.

Turbines	Ideal (MWh)	Optimized (MWh)	Efficiency (%)
60	7,884,000	7,012,378.441	89%
80	10,512,000	8,979,145.726	85%
100	13,140,000	10,784,278.334	82%
150	19,710,000	14,650,508.363	74%

The results presented in Table 6, graphically represented in Figure 16, demonstrate a clear trend of decreasing efficiency as the number of turbines within the wind farm increases. The 60-turbine configuration achieved the highest efficiency at 89%, indicating a relatively low wake loss effect for this density. As the number of turbines increased to 80, 100, and 150, the efficiency progressively dropped to 85%, 82%, and 74%, respectively. This observed decline in efficiency

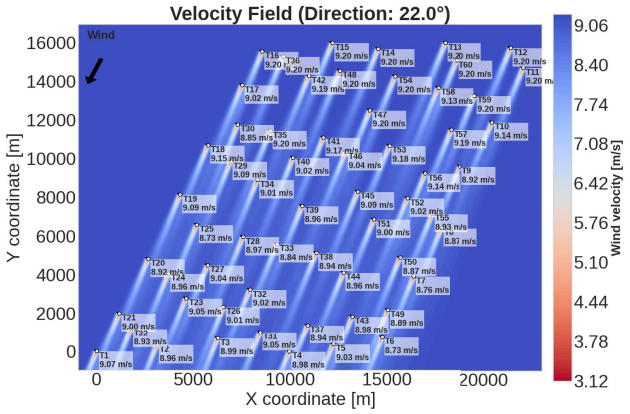

FIGURE 11. Visualization tool for the optimized 60 turbines layout.

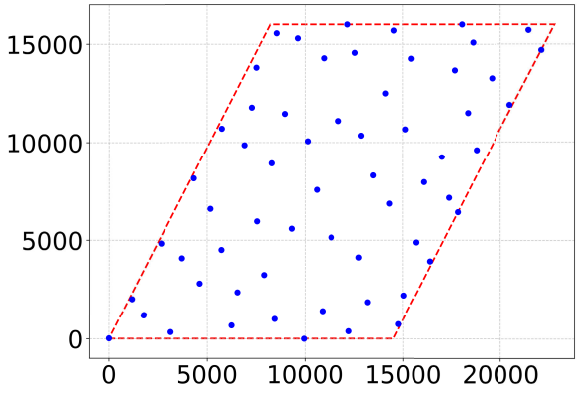

FIGURE 12. Optimized configuration for 60 turbines.

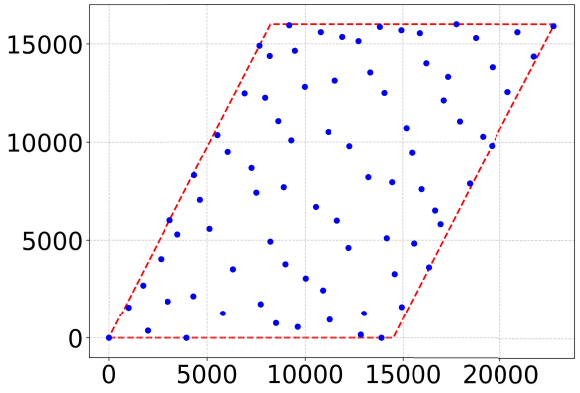

FIGURE 13. Optimized configuration for 80 turbines.

is consistent with the well-understood phenomenon of wake effects in wind farms, where turbines placed downstream experience reduced wind speeds and increased turbulence due to the upstream turbines, leading to a decrease in overall energy capture. Figure 11 demonstrate the wake effect calculated to the 60-turbine optimized configuration.

The optimized layouts, as visually represented in Figures 12 to 15, showcase the algorithm's attempt to mitigate these wake losses by strategically positioning the

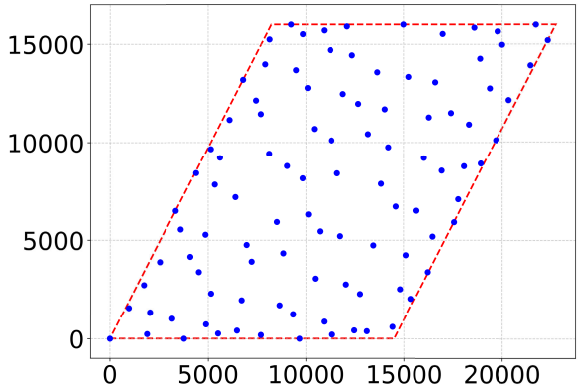

FIGURE 14. Optimized configuration for 100 turbines.

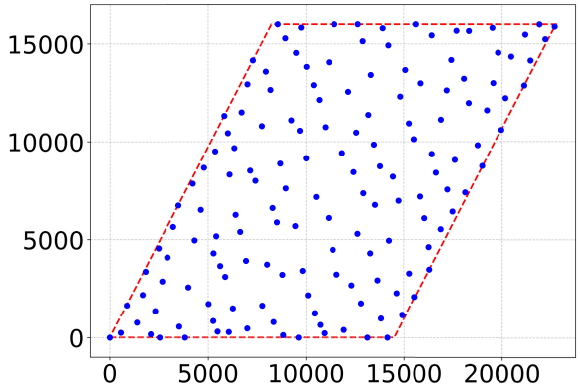

FIGURE 15. Optimized configuration for 150 turbines.

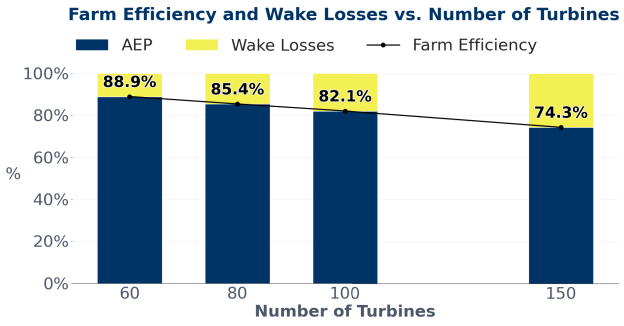

FIGURE 16. Trade-off between number of turbines and wind farm efficiency.

turbines. For lower turbine counts (e.g., 60 and 80 turbines), the optimization algorithm likely found configurations that allowed for greater spacing between turbines or arranged them in patterns that minimized direct wake impingement. However, as the total number of turbines increased and the available area remained constant, the density of turbines inevitably increased, making it more challenging to avoid wake interactions completely. This limitation is reflected in the diminishing returns of the optimization for larger turbine counts.

The visual output from the simulation model, as depicted in Figure 11, provides valuable insight for engineers. This graphical representation allows for a qualitative assessment of the optimized layout and can help identify any potential issues or areas for further refinement that might not be immediately apparent from numerical data alone. For instance, engineers can visually inspect the spacing and alignment of turbines, and wind speed at each turbine, potentially identifying opportunities for minor adjustments to further enhance performance or address practical constraints not fully captured by the optimization model.

It is important to note that the "Ideal (MWh)" values from Table 6 represent a theoretical maximum AEP assuming no wake losses, serving as a baseline for comparison. The difference between the ideal and optimized values quantifies the AEP loss due to wake effects even after optimization. The obtained efficiencies highlight the trade-off between maximizing the number of installed turbines to increase total power output and the inevitable reduction in individual turbine performance due to wake interactions.

VIII. CONCLUSION

In this work, we proposed a modular framework that addresses wind farm layout optimization by decomposing the problem into independent components. This design enables flexible modeling of turbine characteristics, site-specific wind conditions, objective functions, and other relevant parameters. The optimization module is driven by a genetic algorithm that explores potential configurations to identify high-performance layouts based on the configured project data. While the primary focus of this study was the layout optimization of individual candidate areas, the modularity of the framework allows its extension to comparative analyses across multiple sites, turbine models, and configuration constraints. This adaptability positions the framework as a practical and valuable decision-support tool for offshore wind farm development.

To validate the proposed methodology, we applied the framework to a real-world project located near Mostardas-RS on the Brazilian coast. This case study demonstrated the framework's ability to evaluate the maximum AEP for different project sizes, ranging from 60 to 150 turbines, while incorporating the specific characteristics of the site, including historical wind intensity and direction, and the selected turbine model. In addition to numerical results, the framework also provides visualization tools that offer insights into wake interactions and turbine interferences in the optimized layouts, enhancing the interpretability of results and supporting informed decision-making.

In our experimental evaluation, the proposed approach outperformed all other GF methods considered and showed competitive performance compared to gradient-based (G) methods, first place in 16-, 36-turbines cases and thirth place in 64-turbine case benchmarking [4], while maintaining flexibility for incorporating additional design and optimization criteria. In a real-world case study, our approach

demonstrated strong performance, with results ranging from 74% to 89% of efficiency, as shown in Table 6. In future work, we plan to extend the framework to support multi-objective optimization, including economic factors such as installation and maintenance costs, and the design of electrical infrastructure and cabling strategies.

REFERENCES

[1] P. Hou, W. Hu, C. Chen, M. Soltani, and Z. Chen, "Optimization of offshore wind farm layout in restricted zones," *Energy*, vol. 113, pp. 487–496, Oct. 2016.

[2] R. J. Barthelmie, G. C. Larsen, S. T. Frandsen, L. Folkerts, K. Rados, S. C. Pryor, B. Lange, and G. Schepers, "Comparison of wake model simulations with offshore wind turbine wake profiles measured by sodar," *J. Atmos. Ocean. Technol.*, vol. 23, no. 7, pp. 888–901, Jul. 2006.

[3] I. F. Da Silva, T. B. Lazzarin, L. Schmitz, and A. R. Panisson, "Optimizing wind farm project assessments using genetic algorithms," in *Proc. Genetic Evol. Comput. Conf. Companion*, Jul. 2025, pp. 811–814.

[4] N. F. Baker, A. P. J. Stanley, J. Thomas, A. Ning, and K. Dykes, "Best practices for wake model and optimization algorithm selection in wind farm layout optimization," *AIAA Scitech forum*, vol. 2019, p. 540, Jan. 2019.

[5] P. Asaah, L. Hao, and J. Ji, "Optimal placement of wind turbines in wind farm layout using particle swarm optimization," *J. Modern Power Syst. Clean Energy*, vol. 9, no. 2, pp. 367–375, Mar. 2021.

[6] A. Emami and P. Noghreh, "New approach on optimization in placement of wind turbines within wind farm by genetic algorithms," *Renew. Energy*, vol. 35, no. 7, pp. 1559–1564, Jul. 2010.

[7] X. Gao, H. Yang, L. Lin, and P. Koo, "Wind turbine layout optimization using multi-population genetic algorithm and a case study in Hong Kong offshore," *J. Wind Eng. Ind. Aerodynamics*, vol. 139, pp. 89–99, Apr. 2015.

[8] J. J. Thomas, N. F. Baker, P. Malisani, E. Quaeghebeur, S. Sanchez Perez-Moreno, J. Jasa, C. Bay, F. Tilli, D. Bieniek, N. Robinson, A. P. J. Stanley, W. Holt, and A. Ning, "A comparison of eight optimization methods applied to a wind farm layout optimization problem," *Wind Energy Sci.*, vol. 8, no. 5, pp. 865–891, Jun. 2023. [Online]. Available: https://wes.copernicus.org/articles/8/865/2023/

[9] E. Quaeghebeur, R. Bos, and M. B. Zaaijer, "Wind farm layout optimization using pseudo-gradients," *Wind Energy Sci.*, vol. 6, no. 3, pp. 815–839, Jun. 2021.

[10] K. Yang and X. Deng, "Layout optimization for renovation of operational offshore wind farm based on machine learning wake model," *J. Wind Eng. Ind. Aerodynamics*, vol. 232, Jan. 2023, Art. no. 105280.

[11] J. Baptista, B. Jesus, A. Cerveira, and E. J. S. Pires, "Offshore wind farm layout optimisation considering wake effect and power losses," *Sustainability*, vol. 15, no. 13, p. 9893, Jun. 2023.

[12] S. Tao, Q. Xu, A. Feijóo, G. Zheng, and J. Zhou, "Wind farm layout optimization with a three-dimensional Gaussian wake model," *Renew. Energy*, vol. 159, pp. 553–569, Oct. 2020.

[13] L. Cao, M. Ge, X. Gao, B. Du, B. Li, Z. Huang, and Y. Liu, "Wind farm layout optimization to minimize the wake induced turbulence effect on wind turbines," *Appl. Energy*, vol. 323, Oct. 2022, Art. no. 119599.

[14] Z. Liang and H. Liu, "Layout optimization algorithms for the offshore wind farm with different densities using a full-field wake model," *Energies*, vol. 16, no. 16, p. 5916, Aug. 2023.

[15] B. Pérez, R. Mínguez, and R. Guanche, "Offshore wind farm layout optimization using mathematical programming techniques," *Renew. Energy*, vol. 53, pp. 389–399, May 2013.

[16] A. Espejo, R. Mínguez, A. Tomás, M. Menéndez, F. J. Méndez, and I. J. Losada, "Directional calibrated wind and wave reanalysis databases using instrumental data for optimal design of off-shore wind farms," in *Proc. OCEANS IEEE-Spain*, Jun. 2011, pp. 1–9.

[17] G. Mosetti, C. Poloni, and B. Diviacco, "Optimization of wind turbine positioning in large windfarms by means of a genetic algorithm," *J. Wind Eng. Ind. Aerodyn.*, vol. 51, no. 1, pp. 105–116, Jan. 1994.

[18] U. A. Ozturk and B. A. Norman, "Heuristic methods for wind energy conversion system positioning," *Electric Power Syst. Res.*, vol. 70, no. 3, pp. 179–185, Aug. 2004.

[19] S. A. Grady, M. Y. Hussaini, and M. M. Abdullah, "Placement of wind turbines using genetic algorithms," *Renew. Energy*, vol. 30, no. 2, pp. 259–270, Feb. 2005.

[20] P. Lakshmanan, R. Sun, and J. Liang, "Electrical collection systems for offshore wind farms: A review," *CSEE J. Power Energy Syst.*, vol. 7, no. 5, pp. 1078–1092, Sep. 2021.

[21] C. Ng and L. Ran, *Offshore Wind Farms: Technologies, Design and Operation*. Sawston, U.K.: Woodhead Publishing, Mar. 2016.

[22] P. Hou, J. Zhu, K. Ma, G. Yang, W. Hu, and Z. Chen, "A review of offshore wind farm layout optimization and electrical system design methods," *J. Mod. Power Syst. Clean Energy*, vol. 7, no. 5, pp. 975–986, Sep. 2019.

[23] S. J. Andersen, J. N. Sørensen, S. Ivanell, and R. F. Mikkelsen, "Comparison of engineering wake models with CFD simulations," *J. Phys., Conf. Ser.*, vol. 524, Jun. 2014, Art. no. 012161.

[24] J. Wang, Y. L. Mo, B. Izzuddin, and C.-W. Kim, "Exact Dirichlet boundary physics-informed neural network EPINN for solid mechanics," *Comput. Methods Appl. Mech. Eng.*, vol. 414, Sep. 2023, Art. no. 116184.

[25] P. Hou, W. Hu, M. Soltani, and Z. Chen, "A novel energy yields calculation method for irregular wind farm layout," in *Proc. 41st Annu. Conf. IEEE Ind. Electron. Soc.*, Nov. 2015, pp. 380–385.

[26] M. Thørgersen, T. Sørensen, P. Nielsen, A. Grötzner, and S. Chun, "WindPRO/PARK: Introduction to wind turbine wake modelling and wake generated turbulence," EMD International A/S, Aalborg, Denmark, Tech. Rep. 1, 2005.

[27] M. Bastankhah and F. Porté-Agel, "Experimental and theoretical study of wind turbine wakes in yawed conditions," *J. Fluid Mech.*, vol. 806, pp. 506–541, Nov. 2016.

[28] J. J. Thomas and A. Ning, "A method for reducing multi-modality in the wind farm layout optimization problem," *J. Phys., Conf. Ser.*, vol. 1037, Jun. 2018, Art. no. 042012.

[29] N. O. Jensen, "A note on wind generator interaction," Risø National Laboratory, Roskilde, Denmark, Tech. Rep. 2411, 1983.

[30] J. Nocedal and S. J. Wright, *Numerical Optimization* (Springer Series in Operations Research). New York, NY, USA: Springer, 1999.

[31] T. Baeck, D. Fogel, and Z. Michalewicz, Eds., *Evolutionary Computation 1: Basic Algorithms and Operators*, 1st ed., Boca Raton, FL, USA: CRC Press, 2000.

[32] H. M. Pandey, A. Chaudhary, and D. Mehrotra, "A comparative review of approaches to prevent premature convergence in GA," *Appl. Soft Comput.*, vol. 24, pp. 1047–1077, Nov. 2014.

[33] F.-A. Fortin, F.-M. D. Rainville, M.-A. Gardner, M. Parizeau, and C. Gagné, "DEAP: Evolutionary algorithms made easy," *J. Mach. Learn. Res.*, vol. 13, no. 1, pp. 2171–2175, Jul. 2012.

[34] J. Cohen, *Statistical Power Analysis for the Behavioral Sciences*, 2nd ed., Hillsdale, NJ, USA: Lawrence Erlbaum Associates, 1988.

[35] F. Faul, E. Erdfelder, A.-G. Lang, and A. Buchner, "G power 3: A flexible statistical power analysis program for the social, behavioral, and biomedical sciences," *Behav. Res. Methods*, vol. 39, no. 2, pp. 175–191, May 2007.

[36] IBAMA. (2024). *COMPLEXOS EÓLICOS OFFSHORE: PROJETOS COM PROCESSOS DE LICENCIAMENTO AMBIENTAL ABERTOS NO IBAMA*. [Online]. Available: https://www.gov.br/ibama/pt-br/assuntos/laf/consultas/arquivos/20240507_Usinas_Eolicas_Offshore.pdf

[37] E. Gaertner et al., "IEA wind TCP task 37: Definition of the IEA 15-megawatt offshore reference wind turbine," Nat. Renew. Energy Lab. (NREL), Golden, CO, USA, Tech. Rep., 2020.

ITALO FIRMINO DA SILVA is currently pursuing the B.S. degree in computer engineering with the Federal University of Santa Catarina, Araranguá, Santa Catarina, Brazil. He is a Researcher with the Department of Computing, Federal University of Santa Catarina, and a member of the Autonomous Intelligent Agents Laboratory (LAIA). He is also the President of the Academic League of Artificial Intelligence (LIA), where he contributes to promoting integrative and interdisciplinary learning experiences in artificial intelligence. His research interests include evolutionary optimization algorithms (genetic algorithms), numerical simulation, multi-agent systems, and machine learning.

TELLES BRUNELLI LAZZARIN (Senior Member, IEEE) received the B.Sc., M.Sc., and Ph.D. degrees in electrical engineering from the Federal University of Santa Catarina (UFSC), Florianópolis, Brazil, in 2004, 2006, and 2010, respectively. In 2006, he worked with industry, including research and development activities with WEG Motor Drives and Controls, Brazil. He was a Postdoctoral Fellow with UFSC, in 2011, and a Visiting Researcher with Northeastern University, Boston, MA, USA, from 2017 to 2018. He is currently an Associate Professor with the Department of Electrical and Electronics Engineering, UFSC. He is a member of Brazilian Power Electronics Association (SOBRAEP), the Power Electronics Society (PELS), the Industry Applications Society (IAS), and the Industrial Electronics Society (IES). He has been an Associate Editor of *Journal of Power Electronics* (Brazil) and IEEE Open Journal of Power Electronics (OJ-PEL), since 2020.

LENON SCHMITZ (Member, IEEE) received the B.S., M.S., and Ph.D. degrees in electrical engineering from the Federal University of Santa Catarina (UFSC), Florianópolis, Santa Catarina, Brazil, in 2013, 2015, and 2020, respectively. He is currently an Assistant Professor with the Department of Electrical and Electronics Engineering, UFSC. His research interests include high-efficiency power converters, design optimization techniques, and grid-connected systems. He is a member of Brazilian Power Electronics Association (SOBRAEP), the Power Electronics Society (PELS), the Industry Applications Society (IAS), and the Industrial Electronics Society (IES).

ALISON R. PANISSON received the B.S. degree in computer science from The University of Passo Fundo, Passo Fundo, Rio Grande do Sul, Brazil, in 2013, and the M.S. and Ph.D. degrees in computer science from the Pontifical Catholic University of Rio Grande do Sul, Porto Alegre, Rio Grande do Sul, in 2015 and 2019, respectively. He is currently an Assistant Professor with the Department of Computing, Federal University of Santa Catarina (UFSC). His research interests include multi-agent systems and distributed artificial intelligence, theory of mind, optimization problems, and computing applied to social good and environmental causes. He is a member of Brazilian Computer Society (SBC) and coordinates the Autonomous Intelligent Agents Laboratory (LAIA) at UFSC.

Coordenação de Aperfeiçoamento de Pessoal de Nível Superior (CAPES) - ROR identifier: 00x0ma614